Review

Virtual Hemodynamic Assessment of Coronary Lesions: The Advent of Functional Angiography and Coronary Imaging

Sotirios Nikopoulos * , Michael Papafaklis , Panagiota Tsompou , Panagiotis K Siogkas , Antonis I. Sakellarios , Spyros Sioros , Dimitrios I. Fotiadis , Katerina K Naka , Dimitrios N Nikas , Lampros K Michalis

Posted Date: 22 March 2024

doi: 10.20944/preprints202403.1369.v1

Keywords: Cardiovascular disease; Three-dimensional reconstruction; Virtual functional assessment; Medical imaging; Angiography; Computational fluid dynamics

 doi:10.20944/preprints202403.1369.v1

Review

Virtual Hemodynamic Assessment of Coronary Lesions: The Advent of Functional Angiography and Coronary Imaging

Sotirios Nikopoulos [1] *, Michael Papafaklis[4] , Panagiota Tsompou[2,3], Panagiotis Siogkas [2,3] , Antonis Sakellarios[2,3], Spyros Sioros[1], Dimitrios I Fotiadis[2,3], Katerina K Naka[1], Dimitrios Nikas[1] and Lampros Michalis[1]

[1] Department of Cardiology, Medical School, University of Ioannina, 45110 Ioannina, Greece.
[2] Department of Biomedical Research, Institute of Molecular Biology and Biotechnology-FORTH, University Campus of Ioannina, 45115 Ioannina, Greece.
[3] Unit of Medical Technology and Intelligent Information Systems, Department of Materials Science and Engineering, University of Ioannina, 45110 Ioannina, Greece.
[4] Department of Medicine-Interventional Cardiology, University of Patras, Greece
* Correspondence: soternikopoulos@gmail.com

Abstract: Fractional flow reserve (FFR) is well recognized as a gold standard measure for the estimation of functional coronary stenosis. Technological progressions in image processing have empowered the reconstruction of three-dimensional models of the coronary arteries via both non-invasive imaging modalities, such as Coronary Computed Tomography Angiography (CCTA), and invasive coronary angiography or intravascular imaging. The application of computational fluid dynamics (CFD) techniques to coronary 3D anatomical models allows the virtual evaluation of the hemodynamic significance of a coronary lesion with high diagnostic accuracy in comparison to the invasive FFR using pressure wires. These opportunities providing hemodynamic information based on anatomy have given rise to a new era of functional angiography and coronary imaging. However, further validations are needed to overcome several scientific and computational challenges before these methods are applied in everyday clinical practice. This review aims to present all the data on the studies and methodologies that have been presented for the virtual estimation of FFR, and the diagnostic execution of the virtual tools for the hemodynamic assessment of coronary lesions compared to the invasive FFR.

Keywords: cardiovascular disease; three-dimensional reconstruction; computational fluid dynamics; virtual functional assessment; medical imaging; angiography

1. Introduction

Coronary artery disease (CAD) is the main cause of morbidity and mortality around the world [1]. Coronary revascularization by percutaneous coronary intervention (PCI) restores epicardial flow and aims at relieving angina and myocardial ischemia. Recent studies have revealed that in patients with chronic coronary artery disease, the option of whether to perform PCI in moderate lesions is difficult, as both visual assessment and quantitative coronary analysis (QCA) has revealed low correlation with functional stenosis severity [2, 3]. Therefore, the need of evaluating both functional and anatomical severity of obstructive CAD, especially when intermediate stenosis are present, has prompted the adoption of invasive functional indices, principally fractional flow reserve. FFR has enabled interventional specialists to precisely decide which lesions are functionally significant and thus may lead to ischemia and future adverse events [4, 5]. The clinical importance of FFR assessment measured by an intracoronary pressure wire has been acknowledged in the international guidelines and long-term data have shown improved outcomes with FFR-guided decision-making. During the

 doi:10.20944/preprints202403.1369.v1

last decade the use of FFR has slowly raised from 14.8% to 18.5% in patients with angiographically intermediate stenosis [6]. However, its use remains rather limited in everyday clinical practice. This distinction may be related to the invasive nature of FFR evaluation, the prolongation of the cardiac catheterization, the use of hyperemic agents and the high equipment and pharmacologic cost [7]. To overcome these limitations, new methodologies for assessing physiological indices based on fluid mechanics principles have been advanced to reduce the interventional feature of FFR methodology estimation. The progress of technology has also allowed the wide-range application of computational fluid dynamics techniques to coronary imaging, thereby enabled the accurate estimation of the severe occlusions of coronary arterial lesions [8]. During the last decade, these techniques have been applied both to non-invasive (i.e., coronary computed tomography angiography [CCTA]) and invasive (angiography or intravascular imaging in the catheterization laboratory) coronary imaging datasets. All methods make various assumptions for computing equivalent FFR values and demonstrate high diagnostic performance and discriminatory power. The current review summarizes the computational models based on invasive and non-invasive imaging, the application of virtual indices in clinical studies and their performance against the gold- standard FFR, and discusses the future steps and opportunities for incorporating virtual functional assessment into the management strategy of high cardiovascular risk patients.

2. Fluid Mechanics and Computational Fluid Dynamics

To assess the hemodynamic conditions in the cardiovascular system, it is required to take into account the fluid properties and the blood flow characteristics and then apply the universal laws of fluid mechanics [8, 9]. Blood flow in the circulation system is considered as incompressible and is characterized by pulsatility. The arterial walls are distensible, and coronary arteries are displaced and distorted because of the heart beating. The main fluid properties are the density and viscosity which can either be considered as constant (i.e., Newtonian fluid) for simplicity or may be more accurately described by an apparent viscosity value which changes non-linearly due to the applied stress (i.e., non-Newtonian fluid) [10]. The impact of the pressure cut within the stenosis occurs mostly because of the frictional losses arising from the entrance variations (entrance effects) and the kinetic energy loss derived from lumen expansion that yields zones of recirculation. The calculation of the pressure loss can be estimated according to the laws of Bernoulli and Poiseuille and is highly associated with various factors, including the culprit lesions, the area and the range of the stenosis, flow, and the coefficients of expansion loss [10]. In addition, each stenosis characteristic, including the morphology and eccentricity of the stenotic lumen, along with the arterial curvature of the stenotic segment has a tremendous impact on the translational hemodynamics [10]. The computational complexity of the mathematical solutions for the blood flow in the human coronary arteries is large and is affected by the three-dimensional (3D) deformable topology and the pulsatile blood flow and limited by certain assumptions (e.g., the Bernoulli equation is valid for inviscid flow, the Poiseuille equation is valid for steady flow). The solution for the accurate calculation of the coronary blood flow is given by the equations of fluid dynamics, Navier-Stokes equations, which are solved for the unknown pressure that varies according to position and time and for the 3 components of blood velocity. Special conditions must be applied to solve the blood flow equations (e.g., steady or pulsatile flow in an idealized cylindrical geometry). For realistic models of the human coronary arteries, require the simultaneous solution of a huge amount of nonlinear partial differential equations and a numerical method to obtain a solution for velocity and pressure at a finite number of points [11]. For a cardiac cycle the above procedure is repeated for thousands of time intervals. The computational fluid dynamics (CFD) methods are defined as the numerical method for fluid dynamics problems. Three key components that together make up the necessary framework are required for developing the CFD models: (i) 3D arterial models derive from medical images, (ii) numerical methods for solving the 3D Navier-Stokes equations, and (iii) application of initial and boundary conditions [12]. Precise 3D reconstructed coronary artery lesions have derived from the existing imaging modalities. This rapid progress has enabled the development of the CFD models that allow blood flow simulation in realistic geometries. To perform numerical simulations, three main steps have to be accomplished: i)

 doi:10.20944/preprints202403.1369.v1

the pre-processing stage, (ii) the solver stage, and (iii) the post-processing stage [13]. The pre-processing stage involves the description of the fluid construction with a mesh solver where the 3D geometry is divided into numerous finite elements. Then, the flowing substance properties and physiscs of the circulated blood are determined in order to puzzle out the defined mathematical model. Blood is assumed to have a density of approximately 1050 kg/m3 and a viscosity of 3.5×10-3 Pa·s following either the Newtonian law (i.e., constant value) or a non-Newtonian model of viscosity. At the inlet of the artery, stable flow can be applied or, alternatively, a flow waveform to mimic the physiological pulsatile flow in coronary arteries. A no-slip condition and no peretration are applied at the walls and a zero pressure profile is commonly applied at the outlet. The second stage involves the modeling of mathematical calculations to solve the equations of fluid dynamics at the nodes of the finite elements. Finally, after the problem is solved, the last stage involves the extraction and analysis of all hemodynamic parameters of interest [11]. The pressure gradient can be computed in 3D reconstructed patient-specific arterial models by the ratio of the computed pressure distal to the stenosis and the pressure at the inlet of the 3D model which corresponds to the aortic pressure [14]. Consequently, the calculation of the pressure gradient under simulated resting or hyperemic (i.e., FFR) conditions depends on the boundary conditions (e.g., resting or hyperemic flow and distal pressure/microcirculatory resistance) applied on the CFD model.

3. Virtual FFR Based on Non-Invasive Imaging

Progression in image modalities have allowed the 3D coronary reconstruction of the coronary tree and the recognition of the culprit lesions via non-invasive image modalities like Computed Coronary Tomography Angiography (CCTA). These developments have allowed the integration of 3D CT-derived anatomical reconstructions with techniques estimating FFR, based on CFD (computational fluid dynamics). Lately, a series of studies have proposed that the assessment of CCTA-based FFR (FFR-CT) might increase the diagnostic accuracy of CCTA. Most of these studies validated its high diagnostic accuracy and revealed its superiority against stenosis assessment only by CCTA, particularly in terms of improved specificity and positive predictive value.

3.1. FFRCT® by HeartFlow: Offsite Computations

The three initial prospective studies DISCOVER-FLOW (2011)[15], DeFACTO (2012)[16], and HeartFlow® NXT (2015)[17, 18] used invasive FFR as the referral guidance and applied the same cut-off for lesion significance (≤0.8) providing proof that this method can be applied in daily practice . CT angiograms were sent to a central core laboratory (Harbor UCLA Medical Center, Los Angeles, California,USA) for blinded interpretation using an 18-segment coronary model. Three-dimensional models of the coronary anatomy were reconstructed with custom methods applied to CCTA data for simulation of arterial flow and pressure. The FFRCT® methodology is based on three key theories. The first is that arterial supply crosses myocardial demand at rest, the second is that resistance of the microvascular circulation at rest is inversely but not linearly proportional to the dimension of the feeding vessel and the last is that microcirculation reacts predictably to maximum hyperemic condition in case studies with no coronary stenosis. Initially FFRCT® study, DISCOVER FLOW study [15] included 103 patients (159 vessels) with an occlusion in a major coronary lesion and the diagnostic performance of FFRCT® and CCTA were compared. Single vessel analysis, accuracy, specificity, sensitivity, positive predictive value, and negative predictive value for FFRCT® and CCTA were 84, 88, 82, 74, and 92%, respectively. This study crossed its primary end point to reveal a relative upgrade in diagnostic accuracy of ≥25% for FFRCT® when compared with CCTA stenosis. A year later, a larger multicenter study [16] (DeFACTO) concluded 615 vessels where CT, FFRCT®, invasive coronary angiography, and invasive FFR was applied. Notably 150 vessels of moderate stenosis by CT, defined as 30% to 69% stenosis were detected. For vessels of moderate stenosis severity specificity, sensitivity, accuracy, positive predictive and negative predictive value of FFRCT were 67%, 74%, 71%, 41%, and 90%, whereas specificity, sensitivity, accuracy, positive predictive value and negative predictive value of CT stenosis were 72%, 34%, 63%, 27%, and 78%. FFRCT® in comparison with CT stenosis revealed a superior distinction and provided high diagnostic accuracy for detection

 doi:10.20944/preprints202403.1369.v1

of ischemia where segments with intermediate stenosis were involved. Particularly, the above results suggest the potential of FFRCT to functionally rule out intermediate ischemic lesions. The diversity among the current study and the previous report [15] was that the present data comprise all stenosis between 30% and 69% stenosis severity. Furthermore, the current data were derived from a large perspective, multicenter study. The other multicenter study [18] (NXT) showed that FFRCT highly upgraded both per-vessel specificity and positive predictive value (60 to 86% and 33 to 67%, respectively), and the specificity and positive predictive value (32% to 84% and 40% to 65%, respectively) compared with CCTA characteristic curve increased from 0.81 to 0.90 (P=0.0008). Similarly, in 235 patients with degree of stenosis from 30% to 70%, the specificity and positive predictive value increased from 32% to 79% and 37% to 63%, respectively, per-patient. In the NXT study, improvements to the physiological models of microcirculatory resistance were applied, which were confirmed in a retrospective evaluation using data from the DISCOVER-FLOW and DeFACTO studies. In this study an advanced proprietary software was used updated proprietary optimizing automation, image quality assessment and image segmentation.

3.2. FFRCT by Other Groups: Onsite Studies

The aforementioned studies required transferring patient image data to an external core laboratory [19]. The calculation and transfer process remains time consuming (around 1 to 4 h) and is less suitable for prompt clinical decision making, which obviously limits the practical utility. As a result less demanding computational approaches in regular workstations have been developed [20]. This allows near real time FFR estimation using workstations at the point of care [21]. Along with FFRCT® reports, there are several studies using CFD algorithms based on local workstations. Renker et al. [22], performed a retrospective study with less than 60 minutes of analysis time and a FFR of < 0.80 as the gold standard . On a per lesion analysis the sensitivity was 85% and 94% , the specificity was 85% and 84%, and the positive and negative predictive value of on FFR- CT were 71% and 93% respectively. On a per-patient basis, characteristic curve was of borderline superiority to CTA alone (0.91 versus 0.78, P=0.078). A single-center workstation-based study with a 20-minute processing time analyzing 96 lesions in 90 patients with invasive FFR of <0.80 as the gold standard was performed by Kruk et al. [23]. They reported 76% sensitivity, 72% specificity, 67% positive predictive value, and 80% negative predictive value compared with 100% sensitivity, 2% specificity, 43% positive predictive, and 100% negative predictive value for CTA alone. The per-vessel accuracy of FFR-CT was beneath than that for DISCOVER-FLOW (84%) or NXT (86%), but higher than in DeFACTO (69%). The main pitfalls of these studies [22, 23] were the limited number of patients and their single center character that is substantially methodologically inferior to the previous multicenter studies[15, 16, 18]. FFRCT® (HeartFlow®) is based on 3D geometric modeling and computationally intense blood flow analysis which require off-site supercomputing power, and boundary conditions are determined by allometric scaling laws and assumptions regarding microvascular resistance. However, Ko et al. [24] presented an alternative technique for FFR-CT with borderline physics exported from anatomic deformation of coronary lumen and aorta and reduced order or 1-dimensional fluid modeling. Arised positive predictive value (74% vs 60%) and specificity (87% vs. 74%) for FFR-CT than for CCTA alone was observed. This novel approach was reported to require short processing time (30 min) using a standard desktop computer. Smaller pilot studies investigated the on-site feasibility of ischemic coronary lesion detection. Donnelly et al.[25] evaluated the diagnostic accuracy of a new on-site FFRCT towards to the invasive derived FFR as the gold standard and determined whether its diagnostic performance is affected by interobserver variations in lumen segmentation. In this prospective study 44 patients were enrolled and both CCTA and invasive coronary angiography (ICA) was performed. Expert readers manually adjusted the semi-automated coronary lesion segmentations for effective diameter stenosis (EDS). They concluded that on-site FFR-CT simulation is feasible and the diagnostic performance of the on-site FFR-CT simulation algorithm does not depend on the readers' semi-automated lumen segmentation adjustments. Additional procedure time was short and acceptable for integration into a clinical service workflow. Another prototype for on-site determination of FFR-CT on a standard personal computer (PC) compared to

 doi:10.20944/preprints202403.1369.v1

invasively measured FFR in patients with suspected CAD was presented by Röther et al. [26]. In a total 71 patients (91 vessels) a cut-off point of ≤0.80 was indicated as hemodynamically stenosis marker. The average calculation time of FFR-CT was 12.4 ± 3.4 min. After importing the imaging from the installed software, coronary imaging centerlines were automatically spotted and the coronary lumen was segmented and then virtual FFR values for the whole epicardial coronary artery system was analysed. The computation was based on a machine learning algorithm that was trained to reproduce the results of an established CFD-approach with a very low runtime on standard hardware [18]. The most significant upgrade compared to the previously mentioned studies [15, 16, 18] using on-site workflows for calculating FFR-CT was the faster average entire processing time for computation of FFR-CT. This is a novel approach where direct comparison between the diagnostic value of FFR-CT analysis versus ICA is presented. Another recent on-site analysis for the direct diagnostic comparison of FFR-CT and ICA with invasive FFR as state of the art in patients with intermediate stenosis on CCTA was held by by Wardziak et al. in 2019[27]. Ninety-six moderate stenoses (50-90%) from 90 cases, with moderate pre-test probability of coronary artery disease, who underwent coronary CCTA were analyzed. The aforementioned pilot studies showed the feasibility of on-site FFR-CT, which was also shown to have higher discriminatory power compared to QCA, visual ICA, CCTA and visual CCTA. A novel assessment based on the CCTA virtual functional assessment index (vFAI) using an automated in-house developed software was tested on intermediate coronary stenoses (>30% and ≤ 90%) compared to the invasively measured FFR [21, 28]. In 63 patients (74 vessels) with chest discomfort and intermediate (20-90%) pre-test likelihood of CAD undergoing CCTA and invasive angiography with FFR calculation, vFAI measurements were applied after 3D reconstruction of the coronary tree and blood simulations utilizing the finite element strategy. The average diversity of calculations (CT-based vFAI vs FFR) was 0.03 (SD=0.033), indicating a short systematic overestimation of the FFR by vFAI. Despite the small overestimation of FFR compared to the aforementioned studies, the diagnostic precision of the above method was not inferior to them. The analysis time needed was 25 min in average, much lower in contrast to that of the present widespread used FFR-CT software [18] and was equivalent to that of the study by Kruk et al. (average of 20 min per case) [23], or of the study by Ko et al. [24] (average of 27 min per case). Another stand- alone computational methodology for non-invasive calculation of FFR was presented by Siogkas et al.[29]. SmartFFR is based on a transient blood flow simulation and its novelty lies in the fact that it can be effectively applied on arterial bifurcations. Furthermore, it has been released as a stand-alone version [29] and a cloud-based platform, as well [30, 31]. Another advantage is that it offers lies on its rapid execution since it does not require more than a couple of minutes [30].In a novel meta-analysis aiming to demonstrate the efficiency of this recently presented SmartFFR index [29], a dataset of 167 patients (202 vessels) was used. The SmartFFR was calculated while both 3D vessel reconstruction and blood flow simulations were performed, with an average execution time of seven minutes. In the net dataset, SmartFFR combined the calculated indexes of the invasively derived FFR, yielding sensitivity and specificity 94.6% and 85.6%, respectively, using a cut-off value 0.83 to identify stenoses with FFR ≤ 0.80. CCTA offers several advantages with respect to single-photon emission computerized tomography (SPECT) and positron emission tomography (PET) which provide essential non-invasive imaging information about the functional assessment of CAD. A prospective head-to-head comparison of FFR-CT with CCTA, PET, SPECT and perfusion imaging for ischemia diagnosis was reported by Driessen et al.[32]. FFR-CT was excellent in diagnosing vessel-specific ischemia in a total of 208 patients who were investigated for CAD. Additionally, Anagnostopoulos et al. [33] tested the relationship of CCTA-based vFAI with regional flow parameters derived by quantitative PET and its utility in the abnormal vasodilating capability in coronary vessels with stenotic lesions at CCTA. In 78 patients, vFAI, stress myocardial blood flow (MBF) and myocardial flow reserve(MFR) were estimated. CCTA-based vFAI was positively correlated with stress MBF ($R = 0.49$, $P < 0.001$ and $R = 0.53$, $P = 0.001$) and with MFR ($R = 0.41$, $P < 0.001$ and $R = 0.39$, $P = 0.004$) for 15O-water and 13N-ammonia-based measurements, respectively. The accuracy of vFAI for predicting abnormal stress MBF in 15O-water studies was like that of CCTA. However, vFAI performed better than CCTA for predicting abnormal MFR. For 15O-water PET studies the per-vessel

 doi:10.20944/preprints202403.1369.v1

specificity and sensitivity was 90.9% and 77.8%, respectively, for predicting a stress MBF≤2.3. For 13N-ammonia the per-vessel sensitivity was 100%, and specificity was 76.9%.The outcome point revealed that when vFAI is combined with anatomical data, the diagnostic accuracy of CCTA is higher. In summary, compared with the off-site studies the major advantage of the on-site calculation of FFR is the reduction of logistic expenses and the vital time saved when it is applied on urgent bases. In addition, smaller expenses might result to a more well-known software of functional lesion estimation. Disadvantages include the fact that there is no independent control over CCTA image quality, which has been identified as a decisive factor influencing the results of CT-derived FFR.

3.3. FFR-CT and Impact on the Decision Making Process

Lately, there have been many studies which explored the clinical endpoints of virtual FFR-CT-guided diagnostic formations compared to usual practice in suspected high risk patients, and provided a more resource-centric approach of the discussion about FFR-CT and its clinical utility [14].The clinical efficiency of a model using FFR-CT to guide decision-making, compared with conventional testing, had been demonstrated in PLATFORM (Prospect Longitudinal Trial of FFR-CT: Outcome and Resource Impact) trial [34]. The aim of this research was to measure the quality of life and financial results of evaluation strategies that use FFR-CT. A total of 584 patients with referring angina were assigned in prospect to perform either usual testing (n = 287) or CCTA/FFRCT (n = 297). The primary endpoint of this study was based on the percentage of those with planned ICA in whom no significant obstructive CAD (no stenosis ≥50% by core laboratory quantitative analysis or invasive FFR ≤0.80) was found at ICA within 90 days. A second endpoint of this study included death, myocardial infarction and unplanned revascularization which were independently and blindly adjudicated. CCTA/ FFR-CT was related to a notably lower rate of ICA showing no obstructive CAD. The recently completed PROMISE [35] and SCOT-HEART [36] trials suggested that an evaluation strategy based on CCTA enrises diagnostic performance, improves efficiency of triage to invasive catheterization, and may reduce radiation exposure in comparison with functional stress testing, and leads to similar rates of cardiac events [37]. They showed that reserving ICA for patients with an FFRCT of ≤0.80 could decrease ICA without ≥50% stenosis by 44%, and increase the proportion of ICA leading to revascularization by 24%. Since the rate of coronary revascularization in PROMISE was doubled by CCTA as opposed to functional testing, this issue is a significant consideration to take into account. The recent FFRCT RIPCORD study [38] study evaluated the impact of FFRCT and demonstrated that the availability of FFRCT results had a substantial effect on the labeling of significant CAD and management of patients compared to coronary CCTA alone. The HeartFlow technology was used for the extraction of FFRCT and 200 patients from the NXT trial were included. Alternation was noticed on the designated executive category compared to CCTA alone in 72 cases (36%) when post FFRCT data were reported. A useful software for decision making support for management of cases with CAD based on reconstruction of atherosclerotic plaque process was developed in the SMARTool system [30]. This was achieved by performing computational modeling of the major process of the atherosclerotic plaque growth. Firstly, a CCTA was acquired and then 3D modeling of the arterial trees was performed. Then, plaque development modeling and boundary conditions were employed to simulate the primary procedure of atherosclerosis (e.g estimation of ESS). The plaque growth model was based on both biological and genetic data of the patient. Also through this system the extraction of vFAI was achieved. Finally, the modeling of the stent deployment was performed. The aforementioned were integrated in a cloud platform, which provides a decision support tool to doctors for stratification, diagnosis, prediction and treatment to promote personalized medicine. The development of FFR-CT and its utilization in this condition holds the efficacy to reduce unnecessary invasive testing and improve outcomes, owing to its notable precision and its unique ability to detect prognostically important but non obstructive CAD [30, 31]. Clinical interpretation of FFR-CT in conjunction with anatomic assessment of CAD by CCTA is dependent on appropriate coronary luminal modeling. Inadequate signal or contrast relative to noise and coronary motion or misalignment artifacts may compromise the ability to conduct FFR-CT analysis. Efforts to improve standardization of reporting are crucial in order to realize the chance of

 doi:10.20944/preprints202403.1369.v1

FFR-CT to positively influence the clinical supervision of individuals suffering from coronary artery disease.

4. Virtual FFR Based on Invasive Imaging

4.1. Invasive Angiography Derived Virtual FFR

4.1.1. Early Pioneer Studies

FFR computation derived from angiographic imaging data alone reveals as the logical extension of the extra information that conventional angiography can provide when a patient arrives to the cath-lab and has the advantage of better image resolution compared to the CCTA. The first in vivo study to present accurate CFD from Coronary based FFR measurements in the coronary circulation was VIRTU-1 (VIRTUal Fractional Flow Reserve Angiography) [39] which included 19 patients with chronic coronary artery disease awaiting elective percutaneous intervention. The computer model they used for virtual FFR assessment from rotational angiographic images was quite complex and required an average time of 24h for analysis. The comparison against invasive FFR showed a significant correlation, while the precision for detecting FFR≤0.8 was 97%. FFR-QCA was presented as a computer model for quick estimation of FFR in lesion with intermediate coronary stenoses [40]. The approach was to create anatomic reconstruction models by 3D-QCA and then apply CFD using the hyperemic flow rate derived by 3D QCA and TIMI frame count as boundary condition. Computation of FFR-QCA was studied in 68 patients (77 patients). Every vessel analysis lasted less than 10 minutes. This model, however, required the use of vasodilators for causing hyperemia (to calculate the hyperemic volumetric flow rate) during ICA. Mean diameter stenosis was 46.6 ± 7.3% and FFR-QCA correlated well with FFR ($r = 0.81$, $p < 0.001$). A fast computational model for assessing the virtual functional assessment index (vFAI) in intermediate coronary lesions based on routine angiographic images without applying induced hyperemia was proposed by Papafaklis et al. [41]. This virtual index was proposed as a reliable alternative to FFR assessment in patients who underwent ICA. In a total of 139 vessels (120 patients) with intermediate lesions assessed by wire-FFR (reference standard: ≤0.80), 3D QCA was performed. The proposed approach used a 3D-QCA model and steady-flow CFD algorithm to calculate the vFAI which was defined as the ratio of distal to proximal pressure over the lesion for flows in the range from 0-4 ml/s, normalized by the ratio over this range for a normal artery. Discrimination ability of vFAI for ischaemia-producing lesions was high (area under the receiver operator characteristic curve [AUC]: 92% [95% CI: 86-96%]). vFAI was superior to standard 3-D QCA in discriminating FFR≤0.80 (AUC: 78% [95% CI: 70–84%]; $p < 0.0001$ compared to vFAI). High specificity sand sensitivity, (88, 90, and 86%, respectively) in predicting FFR ≤0.80 was described and there was a narrow correlation ($r = 0.78$, $p < 0.0001$) and concurrence of vFAI in contrast to wire-FFR (average difference: −0.0039 ± 0.085, $p = 0.59$). The mean total time required for this procedure (3D-QCA and CFD modeling) was nearly exactly 15 minutes per vessel using an off-the-shelf workstation. The prospective multicenter FAVOR Pilot Trial study presented a new virtual tool, namely quantitative flow ratio (QFR) [42]. To minimize the computation time, instead of CFD techniques, simplistic fluid dynamic equations were applied based on early experimental reports of flow through single arterial stenosis models. The FAVOR study (84 vessels in 73 patients with moderate coronary lesions) aimed to identify the finest way to use this tool investigating offline computation of QFR compared with conventional pressure wire based FFR. Three different blood flow models (volumetric flow input conditions) were tested for the calculation of QFR. The first aims to a hyperemic flow velocity of 0.35 m/s (fQFR). On the other side, cQFR predicts hyperemic contrast-flow velocity by using the TIMI frame count from standard coronary angiographic images. Finally, according to the third one, hyperemic flow velocity could be derived by TIMI frame count while adenosine is infused. In routine clinical work, cQFR was recommended as an index. Although the physicians have to manually interact, the total cQFR in-operation computation time was reported as 5 minutes on average. Good correlations rates with FFR were noticed for fQFR, cQFR, and aQFR ($r = 0.69$ [$p < 0.001$]; $r = 0.77$ [$p < 0.001$]; $r = 0.72$ [$p < 0.001$], respectively). Also, accuracy of diagnosis for determining FFR≤0.80 in a per- vessel analysis was the

 doi:10.20944/preprints202403.1369.v1

highest by aQFR (87%; 95% CI: 80 to 94%), followed by cQFR (86%; 95% CI: 78 to 93%) and fQFR (80%; 95% CI: 71 to 89%).

4.1.2. Large Clinical Studies (QFR, FFRangio)

After the early FAVOR Pilot study, QFR was observed to have good diagnostic accuracy and correlation with FFR in larger prospective in-procedure, retrospective and prospective offline studies. The Functional Assessment by Virtual Online Reconstruction (FAVOR) II trials went through a head-to-head comparison of the high diagnostic accuracy of the in-procedure QFR diagnostic performance using the FFR as a reference standard[42,43]. The FAVOR II China study (308 patients enrolled in 5 centers) was the trial to measure the diagnostic precision of QFR [43]. Online analysis of vessel- level QFR had a diagnostic accuracy of 92.7%, and offline analysis of vessel-level QFR had a high diagnostic accuracy of 93.3%. The FAVOR II Europe and Japan study proved the superior specificity and sensitivity of QFR for detection of functionally severe lesions when compared with 3D-QCA using FFR as the reference standard in a sample of 329 patients. An advantage of QFR was the time for the analysis compared to the invasive measurement of FFR. The comparison between QFR and FFR showed a notable variation in time [4.8 min (IQR 3.5-6.0) versus 7.0 min (IQR 5.0-10.0)]. The WIFI II study [44] (Wire-Free Functional Imaging II) was a predefined sub-study of the Dan-NICAD study (Danish Study of Non-Invasive Diagnostic Testing in CAD) with main target point the estimation of the feasibility and performance of QFR. FFR was performed in 292 lesions, and QFR was calculated in 240 lesions. The median QFR was 0.84 (IQR, 0.77-0.89) and there was a major association ($r = 0.70$, $p<0.0001$) and precision (mean difference of 0.01 ± 0.08, $p = 0.08$) compared with FFR. The QFR diagnostic accuracy was in the range of 0.77 to 0.83 (83-87%; $p = 0.002$), i.e., around the diagnostic cut point. The average time to calculate QFR was 266s (IQR 181-332 s), including the time for 2 optimal angiographic acquisitions and QFR calculation [45]. While the clinical interest in the development of a software (Art care) [46] that provides both 3D reconstruction and functional assessment of the coronary arterial tree increases, a state of the art software was developed by Siogkas et al.[46]. This platform provided to clinicians the ability to reconstruct the desired 3D vessel using different imaging modalities (fusion of IVUS and ICA, fusion of OCT and ICA or just ICA). Furthermore, one of the main point of this study was the use of a dedicated method for the calculation of vFAI for the reconstructed model. Thus, offered both anatomic and functional assessment of the culprit vessel. For the validation of this study a comparison process with a commercial reconstruction software (CASS QCA 3D®) was implemented using different metrics such as the volume of the 3D model, the length and the minimum lumen diameter (MLD) as well as the calculated vFAI on eleven coronary arteries. A high connection was noticed among the two methods with Pearson's correlation coefficient (R) measured at 0.99, 0.99, 0.88 and 0.99 respectively. In addition, the automatic lumen indification modality for IVUS and OCT showed a high accuracy compared to the annotations by cardiology experts. In comparison to other publically available software, the proposed system offers several advantages since it is the only one that can utilize all three coronary imaging modalities. Depending on the available modality, different full 3D reconstructions and the ensuing vFAI calculations require different amounts of time. (2 minutes for the 3D-QCA module, 10 minutes for the IVUS-ICA and OCT-ICA modules). Another method, namely FFRangio, has been recently presented for estimating FFR without the use of a coronary pressure wire or hyperemic agent). This model derives from the 3D coronary artery tree reconstruction and the estimation of the resistance and flow across the stenosis. FFRangio is calculated as the ratio of the maximal flow rate in the culprit artery compared with the maximal flow rate in the lesion without stenosis, and was equated with the FFR at the exact point of the pressure wire sensor [47]. A multicenter international trial, the FAST-FFR study [47], was conducted with the assignment of contrasting the accuracy of on-site FFRangio with pressure wire-FFR. For each patient coronary angiography was applied and coronary pressure wire-FFR was measured by operators blinded to FFRangio. Overall, FFRangio's diagnostic accuracy was 92%, and it was noteworthy that this number held true when focusing solely on FFR values between 0.75 to 0.8. Although the virtual assessment of FFR throughout the entire coronary tree is a significant advantage that would assist the widespread physiological coronary lesion estimation, it

 doi:10.20944/preprints202403.1369.v1

is not clear how much is the total time required to calculate FFRangio, including the manual processing time for the entire coronary tree. Witberg et al.[48], analyzed 5 prospective cohorts with 700 lesions from 588 patients (mean age 65 years, 71% men, 40% with acute coronary syndromes) in which FFRangio was compared against the reference standard wire-based FFR. The FFRangio yielded favorable diagnostic performance with an accuracy of 93%. The increased diagnostic accuracy was also consistent among the different subgroups under investigation. Moreover, the C-statistic for the FFRangio was 0.95 which further highlights its discriminatory power which is important in clinical practice. More recently Siogkas et al. [29] introduced a novel hemodynamic index for coronary stenosis, SmartFFR, which was compared with the gold standard FFR. In this study, the SmartFFR was calculated after the 3D reconstruction of the vessel and the blood flow simulation based on a dataset of 98 patients (114 arteries). A small overestimation of the FFR by this index in this occasion gave an average difference of 0.024 ± 0.051 ($p < 0.0001$), where a high correlation was noticed in the diagnostic performance of the proposed index using the established FFR threshold 0.80 (AUC = 0.975, $p < 0.001$).

4.1.3. Outcome-Based Studies

Beyond studies assessing the correlation and diagnostic accuracy of the virtual indices compared to FFR, the next big step would be outcome-based randomized trials. A multicenter blinded, randomized, sham-controlled trial (FAVOR III China) aimed to establish whether a PCI strategy based on QFR compared to the usual strategy based on angiography for decision-making could yield better results. In FAVOR III China [49] the patients (3847) and all post-interventional specialists and researchers were screened to randomization allocation. In order to control participant masking, patients in both groups wore music-playing headphones during the process and had a preset 10- min delay for real or sham QFR calculation before PCI. A masking questionnaire was delivered to every discharged patient, and at 6 months and 1 year post- procedural, to estimate the achievement of randomization concealment and the perception of treatment allocation. Among patients undergoing PCI, a QFR-guided strategy of lesion selection improved 1-year clinical outcomes (myocardial infarction, death from any cause, or ischemia driven revascularization) compared with standard angiography guidance (Kaplan-Meier estimated rate 5,8% in the QFR-guided group versus 8,8% in the angiography-guided group; difference, −3·0% [95% CI −4·7 to −1·4]; hazard ratio 0·65 [95% CI 0·51 to 0·83];p=0·0004), driven by fewer myocardial infarctions and ischemia-driven revascularizations. In the randomized PANDA III trial [4] QFR was retrospectively analyzed from the angiograms of 1,39 patients who were grouped to those having had QFR-consistent treatment (all functionally ischemic vessels[baseline QFR≤0.80] were treated and all non-ischemic vessels [baseline QFR >0.80] were deferred) and to those having had QFR-inconsistent treatment. QFR-consistent PCI was performed on 814 (58.5%) patients overall, whereas QFR-inconsistent PCI was performed on 577 (41.5%) patients. The risk of 2-year MACE was lower in patients receiving QFR-consistent treatment as compared to those receiving QFR-inconsistent treatment (8.4% vs. 14.7%; hazard ratio [HR] 0.56 [95% CI, 0.41-0.78). About 60% of patients in this post hoc analysis of an all-comers PCI trial received treatment in line with what a QFR measurement would have suggested, and achieving this was linked to better 2-year clinical outcomes.

4.1.4. Discrepancy Versus FFR

Observational data reveal more discordance between QFR and FFR in patients with previous MI, diabetes, kidney disease, previous MI, severe stenosis (high percentage diameter or long lesion length stenosis), and severe aortic stenosis (aortic valve area <0.60 m2). However, the entire validation exported data appeared comparable and promising. In addition, heterogeneous results was compared to non-invasive imaging with QFR. An elevated distal microvascular resistance and impaired ability to dilate the microvasculature could get involved to the reported QFR vs. FFR discordance rate observed in patients with diabetes, previous MI, and microcirculatory dysfunction. However, it is uncertain which index imports a “real” calculation of the epicardial lesion severity in

 doi:10.20944/preprints202403.1369.v1

the setting of increased microvascular resistance, because FFR is inherently affected by microvascular dysfunction.

4.2. Virtual FFR Based on Intravascular Imaging

Efforts to examine the accuracy of virtual functional assessment of coronary lesions using 3D coronary artery reconstruction based on intravascular ultrasound (IVUS) against the invasively measured FFR have been recently reported [29, 46]. A software platform that offered clinicians the ability to calculate the vFAI [41] through CFD simulations based on 3D models derived by the fusion of IVUS and ICA, on a short time, was presented by Siogkas *et al*.[46]. The derived 3D model was represented and then applied to blood flow simulations, resulting to the calculation of vFAI [31]. Seike et al. [50] retrospectively analyzed 50 lesions in 48 patients with coronary stenosis who underwent IVUS and FFR at the same location. The metric called IVUS-FFR was calculated using an algorithm, which was based on a simplified equation (Poiseuille resistance). The average percent diameter stenosis detected on QCA and mean FFR was 56.4±10.7% and 0.69±0.08. IVUS-FFR had a higher linear association with FFR (R=0.78, P<0.001) than what IVUS-derived minimum lumen area (MLA)had (R=0.43, P=0.002). IVUS-FFR was estimated based on normal coronary circulation and many disorders such as hypertrophic cardiomyopathy, LV hypertrophy and valvular disease were absent. Therefore, to precisely evaluate patients with these disorders, further investigation is needed. Another pilot study by Siogkas et al. [28] investigated the feasibility and diagnostic performance of IVUS-based vFAI against FFR. Twenty-two patients underwent IVUS and FFR, with 5 patients presented FFR ≤0.80. The obtained IVUS-based geometries were processed with CFD techniques to calculate the vFAI as previously presented [41]. As a result, great concordance among IVUS-based vFAI and FFR was noticed. The proposed method provides physiologic and anatomic data, as a result enabling complete and comprehensive estimation of coronary vessels pre- and post- intervention using an intravascular imaging catheter without requiring the pressure wire. OCT is used for anatomic and morphological assessment of coronary lesions and provides lumen measurements with excellent reproducibility. OCT also provides information about plaque vulnerability, calcification, and other parameters which helps in guiding the procedure along with diagnostics [51]. These particular properties were used by Art care [46], a multimodality software from which the vFAI index was calculated using the 3D models derived from the fusion of OCT and ICA. The luminal and outer borders were automatically annotated in the OCT frames, then the software utilizes the luminal borders from the centerline extraction module and creates the respective contours for the final 3D model. The 3D model that created can be subjected to computational blood flow simulations with the material properties for blood (i.e., density and viscosity) having been defined by the user. Finally, the required blood flow simulations were performed, in order to calculate the vFAI. Zafar et al. [52] investigated the potential of OCT-derived FFR for the estimation of culprit coronary lesions (stenosis were labeled severe if FFR ≤ 0.8.). The thesis of this study was to assess the blood flow rate and velocity in coronary tree stenosis, calculated through the volumetric analysis of frequency domain optical coherence tomography (FD-OCT) pull back images of the vessel segments, and investigate the corellation between FD-OCT extracted measurements and FFR. This study contained a total of 26 coronary stenosis in 20 patients with stable angina and/or ischemia documented on exercise stress test were studied consecutively with QCA, pressure derived FFR, and OCT during diagnostic coronary angiography. There was a intermediate but significant matching among pressure derived FFR and OCT-derived FFR (r = 0.69, P < 0.001). Bland-Altman report revealed that the average differences between pressure derived FFR and OCT-derived FFR were 0.05 ± 0.14 (limits of agreement: -0.09 to 0.19). The variation in FFR between pressure-derived FFR and FD-OCT-derived FFR was found to have a root mean square error (RMSE) of 447 ± 0.087 FFR units. OCT-derived FFR has the probability to become a valid tool for the evaluation of coronary artery stenosis. In a larger study performed by Ha et al. [53], ninety-two patients with moderate lesion stenosis in the left anterior descending artery received both FFR assessment with OCT performance and pressure wires. The computational FFR calculation was achieved by a CFD algorithm based on OCT data (FFR-OCT). FFR-OCT had 88% diagnostic accuracy

 doi:10.20944/preprints202403.1369.v1

using the wire-based FFR 0.80 cut-off as reference. FFR-OCT also had a stronger correlation with FFR measurements (r = 0.89, p <0.001) than QCA-percent diameter stenosis (r = −0.65, p <0.001), and OCT measurements of minimum lumen area (r = 0.68, p <0.001) and percent area stenosis (r = −0.70, p <0.00 Wei Yu, et al. [54] presented a novel method for estimating FFR from OCT (OFR). A total of 143 vessels from 135 patients were analyzed in the catheterization laboratory. The analysis included patients who underwent both OCT and FFR prior to intervention. The OFR at each position along the culprit vessel was computed based on a validated method derived from a computational FFR model, applying a virtual volumetric flow rate at the inlet boundary. The hyperemic volumetric flow rate was computed by multiplying the proximal reference lumen area from OCT by a virtual hyperemic flow of 0.35 m/s. Following analysis, the calculated OFR values were used to color-code the reconstructed artery, and the OFR value at the most distal point was used to compare it to the FFR. On a off-the-shelf workstation, the average reconstruction time from the point at which the OCT image pullback was entered into the software program until the OFR computation was completed was 55±23 seconds. The per-vessel diagnostic accuracy of OFR was 90% (95% CI: 84% to 95%) using the FFR as gold standard method. OFR has potential for optimizing complex PCI procedures. In addition, OFR is not reliant on angiographic imaging which could be challenging to identify in complex coronary anatomy. Furthermore, the shorter and more automated analysis time for OFR is also suitable for routine use in the laboratory. Fusion of angiographic and OCT data has also been used as the basis for virtually deriving FFR [46, 51]. Pulsatile non-Newtonian coronary flow was simulated using CFD techniques to virtually derive FFR [55]. Virtual FFR could also be co-registered along the OCT pullback segment providing a screenshot of the vFFR that was positively associated with beneficial characterization of the plaque burden.

5. Functional Angiography and Coronary Imaging: Future Perspectives

During the last decade, fluid mechanics algorithms and CFD techniques have a wide application on virtual evaluation of moderate coronary stenosis using both invasive and noninvasive coronary imaging. A large number of validation studies have been performed and have shown that virtual indices have a strong correlation with pressure-wire derived FFR. Newer methods have overcome the obstacle of the off-site analysis and have allowed a faster on-site calculation, presenting a new era of functional angiography. Could the virtual functional tools replace pressure-wire derived FFR? Several studies have shown high but not optimal correlations versus the gold standard. Therefore, additional research is required in order to validate invasive and non-invasive methods of virtual functional assessment of coronary arteries using clinical outcome studies in patients with simple and complex CAD. Pitfalls of the present methodologies are not uncommon and need future improvements. Despite the limitations mentioned, FFR-CT could potentially become the most efficient gate-keeper for invasive investigations, providing not only a reliable 3D reconstruction of coronary anatomy but also a complete hemodynamic assessment of the coronary tree. Angiography-derived FFR provides a lumenogram with higher spatial resolution than CCTA, but still ICA is not free of pitfalls. Further research is needed in order to validate the clinical potential of angiography-derived FFR to provide a quick (i.e., on-line; at the time of catheterization) and reliable alternative to FFR, obviating the need for the pressure-wire and drug-induced hyperemia. The latest randomized trials showing that a QFR-guided PCI strategy resulted in a superior clinical outcome compared to the standard angiography-guided PCI provides data for consideration within the context of the guidelines.

6. Conclusions

FFR is the gold standard for the detection of ischemia-inducing coronary stenosis. Improved clinical outcomes and reduction of repeat revascularization is associated with FFR-guided PCI . Virtual functional assessment acquired by coupling different imaging techniques with fluid mechanics algorithms or CFD models is an attractive alternative to invasive FFR. Various studies during the last decade have presented hemodynamic indices derived from both invasive and non-invasive imaging which showed great correlation against the pressure-wire derived FFR. New

 doi:10.20944/preprints202403.1369.v1

algorithm-based fluid models have been introduced and contribute to a path toward patient-tailored treatment strategies which are based on the combination of physiology and anatomy for complete and comprehensive assessment of coronary stenosis. However, numerous scientific and logistical pitfalls must be overcome in order to enter in our routine clinical practice these computational approaches

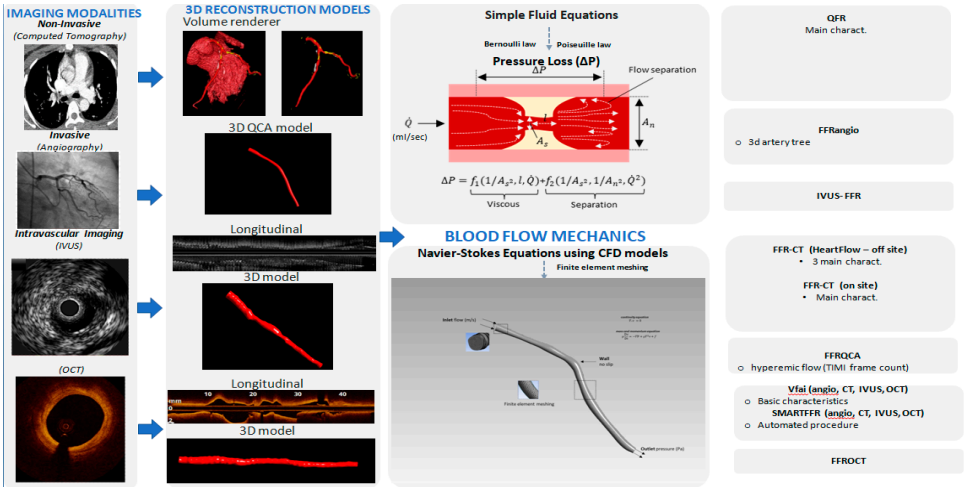

Figure 1.

Funding: This research received no external funding

Conflicts of Interest: The authors declare no conflicts of interest

References

1. Mangla A, Oliveros E, Williams KA, Sr., Kalra DK. Cardiac Imaging in the Diagnosis of Coronary Artery Disease. Current Problems in Cardiology. 2017; 42: 316-366.
2. McCullough PA. Coronary artery disease. Clin J Am Soc Nephrol. 2007; 2: 611-616.
3. Knuuti J, Wijns W, Saraste A, Capodanno D, Barbato E, Funck-Brentano C, et al. 2019 ESC Guidelines for the diagnosis and management of chronic coronary syndromes. Eur Heart J. 2020; 41: 407-477.
4. Zhang R, Dou K, Guan C, Zou T, Zhang M, Yuan S, et al. Outcomes of quantitative flow ratio-based percutaneous coronary intervention in an all-comers study. EuroIntervention. 2022; 17: 1240-1251.
5. Schampaert E, Kumar G, Achenbach S, Galli S, Tanaka N, Teraphongphom T, et al. A global registry of fractional flow reserve (FFR)-guided management during routine care: Study design, baseline characteristics and outcomes of invasive management. Catheter Cardiovasc Interv. 2020; 96: E423-e431.
6. Parikh RV, Liu G, Plomondon ME, Sehested TSG, Hlatky MA, Waldo SW, et al. Utilization and Outcomes of Measuring Fractional Flow Reserve in Patients With Stable Ischemic Heart Disease. J Am Coll Cardiol. 2020; 75: 521
7. Fearon WF, Bornschein B, Tonino PA, Gothe RM, Bruyne BD, Pijls NH, et al. Economic evaluation of fractional flow reserve-guided percutaneous coronary intervention in patients with multivessel disease. Circulation.2010; 122: 2545-2550.
8. Carvalho V, Pinho D, Lima RA, Teixeira JC, Teixeira SJF. Blood Flow Modeling in Coronary Arteries: A Review.2021; 6: 53.
9. Kannojiya V, Das AK, Das PK. Simulation of Blood as Fluid: A Review From Rheological Aspects. IEEE528 Rev Biomed Eng. 2021; 14: 327-341.
10. Papafaklis MI, Mavrogiannis MC, Siogkas PK, Lakkas LS, Katsouras CS, Fotiadis DI, et al. Functional assessment of lesion severity without using the pressure wire: coronary imaging and blood flow simulation. Expert Review of Cardiovascular Therapy. 2017; 15: 863-877.
11. Vardhan M, Randles AJBR. Application of physics-based flow models in cardiovascular medicine: Current practices and challenges. Biophysics Reviews. 2021; 2: 011302.
12. Zhong L, Zhang JM, Su B, Tan RS, Allen JC, Kassab GS. Application of Patient-Specific Computational Fluid Dynamics in Coronary and Intra-Cardiac Flow Simulations: Challenges and Opportunities. Front Physiol. 2018; 536 9: 742.
13. Kim HJ, Vignon-Clementel IE, Coogan JS, Figueroa CA, Jansen KE, Taylor CA. Patient-specific modeling of blood flow and pressure in human coronary arteries. Ann Biomed Eng. 2010; 38: 3195-3209.

14. Chinnaiyan KM, Safian RD, Gallagher ML, George J, Dixon SR, Bilolikar AN, et al. Clinical Use of CT-Derived Fractional Flow Reserve in the Emergency Department. JACC: Cardiovascular Imaging. 2020; 13: 452-461.
15. Koo BK, Erglis A, Doh JH, Daniels DV, Jegere S, Kim HS, et al. Diagnosis of ischemia-causing coronary stenoses by noninvasive fractional flow reserve computed from coronary computed tomographic angiograms. Results from the prospective multicenter DISCOVER-FLOW (Diagnosis of Ischemia-Causing Stenoses Obtained Via Noninvasive Fractional Flow Reserve) study. J Am Coll Cardiol. 2011; 58: 1989-1997.
16. Nakazato R, Park HB, Berman DS, Gransar H, Koo BK, Erglis A, et al. Noninvasive fractional flow reserve derived from computed tomography angiography for coronary lesions of intermediate stenosis severity: results from the DeFACTO study. Circulation: Cardiovascular Imaging. 2013; 6: 881-889.
17. Gaur S, Achenbach S, Leipsic J, Mauri L, Bezerra HG, Jensen JM, et al. Rationale and design of the HeartFlowNXT (HeartFlow analysis of coronary blood flow using CT angiography: NeXt sTeps) study. J Cardiovasc550 Comput Tomogr. 2013; 7: 279-288.
18. Nørgaard BL, Leipsic J, Gaur S, Seneviratne S, Ko BS, Ito H, et al. Diagnostic performance of noninvasive fractional flow reserve derived from coronary computed tomography angiography in suspected coronary artery disease: the NXT trial (Analysis of Coronary Blood Flow Using CT Angiography: Next Steps). Journal of the American College of Cardiology. 2014; 63: 1145-1155.
19. Zhuang B, Wang S, Zhao S, Lu M. Computed tomography angiography-derived fractional flow reserve (CT-FFR) for the detection of myocardial ischemia with invasive fractional flow reserve as reference: systematic review and meta-analysis. European Radiology. 2020; 30: 712-725.
20. Hecht HS, Narula J, Fearon WF. Fractional Flow Reserve and Coronary Computed Tomographic Angiography: A Review and Critical Analysis. Circulation Research. 2016; 119: 300-316.
21. Siogkas PK, Anagnostopoulos CD, Liga R, Exarchos TP, Sakellarios AI, Rigas G, et al. Noninvasive CT-based hemodynamic assessment of coronary lesions derived from fast computational analysis: a comparison against fractional flow reserve. European Radiology. 2019; 29: 2117-2126.
22. Renker M, Schoepf UJ, Wang R, Meinel FG, Rier JD, Bayer RR, 2nd, et al. Comparison of diagnostic value of a novel noninvasive coronary computed tomography angiography method versus standard coronary angiography for assessing fractional flow reserve. Am J Cardiol. 2014; 114: 1303-1308.
23. Kruk M, Wardziak Ł, Demkow M, Pleban W, Pręgowski J, Dzielińska Z, et al. Workstation-Based Calculation of CTA-Based FFR for Intermediate Stenosis. JACC: Cardiovascular Imaging. 2016; 9: 690-699.
24. Ko BS, Cameron JD, Munnur RK, Wong DTL, Fujisawa Y, Sakaguchi T, et al. Noninvasive CT-Derived FFR Based on Structural and Fluid Analysis: A Comparison With Invasive FFR for Detection of Functionally Significant Stenosis. JACC: Cardiovascular Imaging. 2017; 10: 663-673.
25. Donnelly PM, Kolossváry M, Karády J, Ball PA, Kelly S, Fitzsimons D, et al. Experience With an On-Site Coronary Computed Tomography-Derived Fractional Flow Reserve Algorithm for the Assessment of Intermediate Coronary Stenoses. American Journal of Cardiology. 2018; 121: 9-13.
26. Röther J, Moshage M, Dey D, Schwemmer C, Tröbs M, Blachutzik F, et al. Comparison of invasively measured FFR with FFR derived from coronary CT angiography for detection of lesion-specific ischemia: Results from a PC-based prototype algorithm. Journal of Cardiovascular Computed Tomography. 2018; 12: 101-107.
27. Wardziak Ł, Kruk M, Pleban W, Demkow M, Rużyłło W, Dzielińska Z, et al. Coronary CTA enhanced with CTA based FFR analysis provides higher diagnostic value than invasive coronary angiography in patients with intermediate coronary stenosis. Journal of Cardiovascular Computed Tomography. 2019; 13: 62-67.
28. Siogkas PK, Papafaklis MI, Lakkas L, Exarchos TP, Karmpaliotis D, Ali ZA, et al. Virtual Functional Assessment of Coronary Stenoses Using Intravascular Ultrasound Imaging: A Proof-of-Concept Pilot Study. Heart, Lung & Circulation. 2019; 28: e33-e36.
29. [29] Siogkas PK, Lakkas L, Sakellarios AI, Rigas G, Kyriakidis S, Stefanou KA, et al. SmartFFR, a New Functional Index of Coronary Stenosis: Comparison With Invasive FFR Data. Frontiers in Cardiovascular Medicine.585 2021; 8: 714471-714471.
30. Sakellarios AI, Rigas G, Kigka V, Siogkas P, Tsompou P, Karanasiou G, et al. SMARTool: A tool for clinical decision support for the management of patients with coronary artery disease based on modeling of atherosclerotic plaque process. Annu Int Conf IEEE Eng Med Biol Soc. 2017; 2017: 96-99.
31. Sakellarios A, Correia J, Kyriakidis S, Georga E, Tachos N, Siogkas P, et al. A cloud-based platform for the non-invasive management of coronary artery disease. Enterprise Information Systems. 2020; 14: 1102-1123.
32. Driessen RS, Danad I, Stuijfzand WJ, Raijmakers PG, Schumacher SP, van Diemen PA, et al. Comparison of Coronary Computed Tomography Angiography, Fractional Flow Reserve, and Perfusion Imaging for Ischemia Diagnosis. Journal of the American College of Cardiology. 2019; 73: 161-173.
33. Anagnostopoulos CD, Siogkas PK, Liga R, Benetos G, Maaniitty T, Sakellarios AI, et al. Characterization of functionally significant coronary artery disease by a coronary computed tomography angiography-based

 doi:10.20944/preprints202403.1369.v1

index: a comparison with positron emission tomography. European Heart Journal Cardiovascular Imaging. 2019; 20: 897-905.
34. Pontone G, Rabbat MG. The New Era of Computational Fluid Dynamics in CT Angiography: Far Beyond the FFR Number. JACC: Cardiovascular Imaging. 2017; 10: 674-676.
35. Lu MT, Ferencik M, Roberts RS, Lee KL, Ivanov A, Adami E, et al. Noninvasive FFR Derived From 600 Coronary CT Angiography: Management and Outcomes in the PROMISE Trial. JACC Cardiovasc Imaging. 2017; 601 10: 1350-1358.
36. CT coronary angiography in patients with suspected angina due to coronary heart disease (SCOT-HEART): 603 an open-label, parallel-group, multicentre trial. Lancet. 2015; 385: 2383-2391.
37. Adamson PD, Newby DE, Hill CL, Coles A, Douglas PS, Fordyce CB. Comparison of International 605 Guidelines for Assessment of Suspected Stable Angina: Insights From the PROMISE and SCOT-HEART. JACC: 606 Cardiovascular Imaging. 2018; 11: 1301-1310.
38. Curzen NP, Nolan J, Zaman AG, Nørgaard BL, Rajani R. Does the Routine Availability of CT-Derived FFR608 Influence Management of Patients With Stable Chest Pain Compared to CT Angiography Alone?: The FFR(CT) 609 RIPCORD Study. JACC Cardiovasc Imaging. 2016; 9: 1188-1194.
39. Morris PD, Ryan D, Morton AC, Lycett R, Lawford PV, Hose DR, et al. Virtual fractional flow reserve 611 from coronary angiography: modeling the significance of coronary lesions: results from the VIRTU-1 (VIRTUal 612 Fractional Flow Reserve From Coronary Angiography) study. JACC: Cardiovascular Interventions. 2013; 6: 149- 613 157.
40. Tu S, Barbato E, Köszegi Z, Yang J, Sun Z, Holm NR, et al. Fractional flow reserve calculation from 3- 615 dimensional quantitative coronary angiography and TIMI frame count: a fast computer model to quantify the616 functional significance of moderately obstructed coronary arteries. JACC: Cardiovascular Interventions. 2014; 7: 617 768-777.
41. Papafaklis MI, Muramatsu T, Ishibashi Y, Lakkas LS, Nakatani S, Bourantas CV, et al. Fast virtual 619 functional assessment of intermediate coronary lesions using routine angiographic data and blood flow simulation in620 humans: comparison with pressure wire - fractional flow reserve. EuroIntervention : journal of EuroPCR in 621 collaboration with the Working Group on Interventional Cardiology of the European Society of Cardiology. 2014; 622 10: 574-583.
42. Tu S, Westra J, Yang J, von Birgelen C, Ferrara A, Pellicano M, et al. Diagnostic Accuracy of Fast624 Computational Approaches to Derive Fractional Flow Reserve From Diagnostic Coronary Angiography: The 625 International Multicenter FAVOR Pilot Study. JACC: Cardiovascular Interventions. 2016; 9: 2024-2035.
43. Xu B, Tu S, Qiao S, Qu X, Chen Y, Yang J, et al. Diagnostic Accuracy of Angiography-Based Quantitative627 Flow Ratio Measurements for Online Assessment of Coronary Stenosis. Journal of the American College of 628 Cardiology. 2017; 70: 3077-3087.
44. Westra J, Tu S, Winther S, Nissen L, Vestergaard MB, Andersen BK, et al. Evaluation of Coronary Artery630 Stenosis by Quantitative Flow Ratio During Invasive Coronary Angiography: The WIFI II Study (Wire-Free 631 Functional Imaging II). Circulation: Cardiovascular Imaging. 2018; 11: e007107.
45. Yazaki K, Otsuka M, Kataoka S, Kahata M, Kumagai A, Inoue K, et al. Applicability of 3-Dimensional 633 Quantitative Coronary Angiography-Derived Computed Fractional Flow Reserve for Intermediate Coronary Stenosis.634 Circulation Journal. 2017; 81: 988-992.
46. Siogkas PK, Stefanou KA, Athanasiou LS, Papafaklis MI, Michalis LK, Fotiadis DI. Art care: A multi-modality coronary 3D reconstruction and hemodynamic status assessment software. Technology and Health Care. 637 2018; 26: 187-193.
47. Fearon WF, Achenbach S, Engstrom T, Assali A, Shlofmitz R, Jeremias A, et al. Accuracy of Fractional 639 Flow Reserve Derived From Coronary Angiography. Circulation. 2019; 139: 477-484.
48. Witberg G, De Bruyne B, Fearon WF, Achenbach S, Engstrom T, Matsuo H, et al. Diagnostic Performance641 of Angiogram-Derived Fractional Flow Reserve: A Pooled Analysis of 5 Prospective Cohort Studies. JACC: 642 Cardiovascular Interventions. 2020; 13: 488-497.
49. Song L, Tu S, Sun Z, Wang Y, Ding D, Guan C, et al. Quantitative flow ratio-guided strategy versus 644 angiography-guided strategy for percutaneous coronary intervention: Rationale and design of the FAVOR III China 645 trial. Am Heart J. 2020; 223: 72-80.
50. Seike F, Uetani T, Nishimura K, Kawakami H, Higashi H, Fujii A, et al. Intravascular Ultrasound-Derived 647 Virtual Fractional Flow Reserve for the Assessment of Myocardial Ischemia. Circ J. 2018; 82: 815-823.
51. Karanasiou GS, Rigas GA, Kyriakidis SK, Tachos NS, Sakellarios AI, Fotiadis DI. InSilc: 3D 649Reconstruction and plaque characterization tool. Annu Int Conf IEEE Eng Med Biol Soc. 2018; 2018: 4528-4531.
52. Zafar H, Sharif F, Leahy MJ. Feasibility of intracoronary frequency domain optical coherence tomography derived fractional flow reserve for the assessment of coronary artery stenosis. Int Heart J. 2014; 55: 307-311.

 doi:10.20944/preprints202403.1369.v1

53. Ha J, Kim JS, Lim J, Kim G, Lee S, Lee JS, et al. Assessing Computational Fractional Flow Reserve From Optical Coherence Tomography in Patients With Intermediate Coronary Stenosis in the Left Anterior Descending Artery. Circ Cardiovasc Interv. 2016; 9.
54. Yu W, Huang J, Jia D, Chen S, Raffel OC, Ding D, et al. Diagnostic accuracy of intracoronary optical coherence tomography-derived fractional flow reserve for assessment of coronary stenosis severity. EuroIntervention.2019; 15: 189-197.
55. Poon EKW, Thondapu V, Revalor E, Ooi A, Barlis P. Coronary optical coherence tomography-derived 659 virtual fractional flow reserve (FFR): anatomy and physiology all-in-one. Eur Heart J. 2017; 38: 3604-3605.